

## **INFRASONIC SOURCE LOCATION OF THE APRIL 23, 2001, BOLIDE EVENT**

Milton Garces<sup>1</sup>, Claus Hetzer<sup>1</sup>, Kent Lindquist<sup>2</sup>, Roger Hansen<sup>2</sup>, John Olson<sup>3</sup>, Charles Wilson<sup>3</sup>,  
Douglas Drob<sup>4</sup>, and Michael Hedlin<sup>5</sup>

University of Hawaii, Manoa<sup>1</sup>, University of Alaska, Fairbanks<sup>2,3</sup>  
Naval Research Laboratory<sup>4</sup>, and University of California, San Diego<sup>5</sup>

<sup>1,2,4</sup>Sponsored by National Nuclear Security Administration  
Office of Nonproliferation Research and Engineering  
Office of Defense Nuclear Nonproliferation

Contract No. DE-FC04-98AL79801

### **ABSTRACT**

An infrasonic event with a 10- to 15-minute duration was detected by multiple infrasonic arrays on April 23, 2001. Data from infrasound arrays IS59 (Hawaii), FAI (Fairbanks), and IS57 (California) are selected for the determination of the origin time and the location of the infrasonic source. The bolide was not observed by infrasonic stations operating in South America or the South Pacific. There were also no confirmed detections from ocean-bottom seismometers and hydroacoustic sensors near the epicenter. A preliminary location was obtained from array back azimuths, and this location was used as a seed for the source iteration process. We compare the estimates obtained for the source location and origin time using different atmospheric models and different stations. The tau-p method is used to estimate theoretical travel times, and we estimate the source position by reducing the time residuals. The variability in the locations may be due to errors in the atmospheric models, the propagation models, or the array estimates. We outline the algorithm used for the location of infrasonic sources, and assess the accuracy of two- and three-station epicentral determinations.

**KEY WORDS:** infrasound, source location

### **OBJECTIVE**

The aim of this work is to evaluate the precision of infrasonic source locations from multiple array detections. We consider possible modifications to the atmospheric models that may yield consistency between infrasonic locations and satellite-based locations.

### **RESEARCH ACCOMPLISHED**

#### **Introduction**

On April 24, 2001, Rod Whitaker of the Los Alamos National Laboratory reported that an interesting event had been detected by DLIAR on the previous day, April 23. Shortly thereafter, David Brown of the Center for Monitoring Research, issued a message corroborating associated detections by IS10, DLIAR, and IS59. Michael Hedlin and Jon Berger confirmed detection at IS57, Pinon Flat. Charles Wilson, John Olson, and Kent Lindquist provided results from the FAI research array, which will soon become IS53. French stations in Bolivia, French Guyana, and Tahiti did not observe the event, and no evident detections were reported by the seismic sensors and hydrophones deployed at the Hawaii-2 Observatory at 28° N 142° W.

Dr. Brown promptly made available to Defense Threat Reduction Agency (DTRA) researchers CSS data for stations IS10, DLIAR, IS57, IS59, and SGAR, and the Infrasound Laboratory (ISLA) of the University of Hawaii used Matseis, from Sandia National Laboratories, and Infratool, from Los Alamos National Laboratory, to produce rapid estimates of the arrival time, azimuth, and slowness of the signal at these arrays. Preliminary locations were made using the tau-p code presently under development at the ISLA. The authors did not know the source of the April 23 event until June 2001, when the Department of Energy (DOE) issued an official information release.

According to the DOE release, infrared sensors aboard US Department of Defense (DOD) satellites detected the impact of a bolide on 23 April 2001 at 06:12:35 UTC (988006355 Epoch time). The bolide appeared to explode at an altitude of 28.5 km above the coordinates of 27.9 North and 133.89 West. The impact was simultaneously detected by space-based visible wavelength sensors operated by the US DOE. The total energy in the visible band was  $4.6 \times 10^{12}$  joules. The location for the April 23 event determined by the optical systems is referred to as LO1.

Some discrepancies exist between the satellite and the infrasonic locations that would be expected for these events. There are two possible explanations for these discrepancies: either there was more than one bolide impact within a ten-minute window, or our infrasonic and atmospheric models need to be reviewed. We consider the second explanation, and investigate what modifications to the atmospheric models would produce infrasonic travel-time results consistent with the LO1 location. It is also possible that the sound propagation models are incomplete, and that scattering in the troposphere and stratosphere has an important effect.

### **Array Processing of the Infrasonic Data for Selected Stations**

The locations of selected arrays that detected the April 23 event and used in this study are given in Table 1 and shown in Figure 1. These stations were selected because they are the three closest International Monitoring System (IMS) stations to the event. Based on the epicentral location issued by the DOE release, the range of each station to the source and the expected azimuth of the incoming signal can be readily computed. We used a modified version of Infratool and frequency-wavenumber (FK) analysis to estimate the arrival information of the signals observed at each array (Table 2). To obtain these estimates, we first band pass the signal with a Butterworth zero-phase 2<sup>nd</sup> order filter between 0.1 and 1 Hz, and use FK analysis with 101 slowness values on successive 45-second Hamming windowed segments of data. We also compute the correlation and the F-statistic for each window (Figures 2-3). We thus obtain estimates of the incidence azimuth (measured clockwise from North), slowness (in seconds/degree), and onset time of the signal. The onset time is determined from an increase in the F-statistic and correlation, as well as from the time at which azimuth values become stable. The arrival estimates are dependent on the choice of frequency band and time window, and we use the same parameters on all arrays to ensure consistency. Further, the azimuth and slowness of the detected infrasonic waves change with time. Thus, we restrict our estimates to the first arrivals, demarcated by the vertical bar in Figures 2 and 3. The apparent slowness of the signal (travel time divided by range), the apparent speed (range divided by travel time), and the azimuth deviation in the signal (expected azimuth – observed azimuth) are provided in Table 3. A positive azimuth deviation corresponds to a correction to the right of the arrival azimuth.

The azimuth and high slowness values observed at FAI are not very precise because the position of the array elements are only accurate to +/-15 m, and we have data from only three of the four elements. For an array aperture of 1 km, this leads to a maximum error in the apparent horizontal phase velocity of ~6%. Such relatively small errors would still not account for the strong discrepancies in the expected and observed array estimates. The azimuth values obtained at IS59 and IS57 (both arrays have an aperture of ~2 km) are reasonable, but the slowness values at IS57 fluctuate quite a bit. This variability in the slowness at IS57 may be due to its relative proximity to the source, and to possible interference of superposed wave trains. Some of the errors in the slowness and azimuth values obtained at IS59 may be attributed to site effects. At the edge of the slowness plane, the 3-D effects of the array element locations are negligible, but the mountains around IS59 may alter the geometry of the propagating wavefronts. Until these site-specific issues are resolved, the arrival time of the signal provides the most robust parameter for performing the source location.

### **Initial Infrasonic Location Procedure for the April 23 Event**

A preliminary location was made by using intersecting back azimuths from five infrasonic arrays: IS59, IS57, FAI, DLIAR, and IS10. However, the epicenter given by the area of intersection of these lines yielded arrival times inconsistent with atmospheric model predictions. We obtained SAGE meteorological data from the Naval Research Laboratory for the day of April 23, 2001, at most of the sites except DLIAR, which is not near any IMS station. We used the meteorological data for IS57 to infer the arrival times for DLIAR. We then used the tau-p method of Garces et al., (1998) to compute predicted travel times (T), ranges (X), azimuth deviation (in degrees, where positive means a correction to the right of the direction of arrival), effective slowness (T/X), and the height of the atmosphere where the selected rays turn. We then use the Geiger method to reduce the residuals in the arrival times. Various assumptions went into these computations. First, the observed slowness

values in most of the arrays were higher than expected, as some of them did not correspond to acoustic velocities. Such arrivals are not predicted by ray theory, and suggest that scattering may have been significant. We use the highest slowness values that are allowed by the ray models for the specified arrival azimuth at each site. Second, we use the local meteorological conditions at the epicenter to trace rays along a rather long transect, where we know we may experience varying conditions. We expect the first skip to be reasonably accurate, and further skips to degrade in precision. Despite these approximations, self-consistent results were obtained for the epicenter and origin time of the source. However, although the infrasonic location (LA1) was close to the satellite location (LO1), the origin times did not agree. The infrasonic inversion yielded an origin time of 05:58 UT at 29.5 North, 134.9 West, whereas LO1 has an origin time of 06:12:35 UT at 27.9 North and 133.89 West.

#### **Modification of the Atmospheric Model**

The discrepancy of 00:12:37, 1.6° in latitude, and 1° in longitude may be explained by inaccuracies in the atmospheric models, as well as by inadequacies in the ray-tracing formulation. The epicentral location inferred from the infrasonic data is relatively close to LO1, but the origin time is too early. We explore the possibility of modifying the atmospheric models to account for these differences. We concentrate on the travel times, and attempt to match the effective propagation speeds of the arrivals.

The atmospheric profiles used to compute LA1 predicted stratospheric winds that were too weak. As a result, no stratospheric arrivals were predicted for any of the stations, and the location was computed using only the predicted thermospheric arrivals. New atmospheric models were used for this paper, where meteorological estimates up to 55 km were obtained from the NASA Goddard Spaceflight Center (GSFC) Data Assimilation Office. The propagation model parameters are shown in solid lines in the upper panel of Figure 4. Using these profiles, new effective speed values were used to obtain a location and origin time, and this solution is referred to as LA1b. Table 4 shows the propagation model results for this scenario, and the upper panel of Figure 5 shows the location of LA1b.

As shown in Table 4, the apparent speeds for IS59 and FAI computed with an unperturbed atmosphere are too slow to explain the observed arrivals. The source location has also been degraded. The apparent propagation speeds for IS57 are consistent with predictions, which suggest that the atmospheric and sound propagation models along the dominant stratospheric wind direction are adequate. We consider modifications to the upper atmosphere models to account for the discrepancy in the locations. After various iterations, it was observed that the most effective modification involved an increase in the atmospheric sound speed, which implies an increase in the temperature and/or a decrease in the molecular mass.

To modify the atmospheric profiles, a cosine taper was constructed to add a bias at specified height ranges to the wind and temperature profiles. The cosine taper ensures a smooth transition between the unperturbed profile and the perturbed region. The atmospheric profile used in this study was provided by the Naval Research Laboratory (NRL) and was evaluated using a procedure described in Garces et al. (2000). We only concern ourselves with atmospheric heights below 120 km, as most of the rays corresponding to the first arrivals are predicted to turn below this level. In addition, the atmospheric estimates up to 50 km have been validated by various means, and are more accurate than the empirical estimates for heights above 50 km. Thus, we concentrate on the region between 50 km and 120 km, also known as the Mesosphere and Lower Thermosphere (MLT). The selected cosine taper increases from 60 km up to 100 km, where it remains at a constant value. We used the atmospheric profile at the epicenter for our tests. This simplification is reasonable for the E-W line between IS59 and IS57, as the latitude does not change drastically. However, between Fairbanks and the epicentral location, the atmosphere changes quite dramatically. Various perturbations to the atmospheric profile were attempted, and a reasonable fit for all three azimuths was obtained for a 10% increase in the sound speed, with the wind velocity profiles remaining unperturbed. The upper panel of Figure 4 shows the perturbed sound speed profile as a dashed line.

The ratio of the temperature to the molecular mass of the atmosphere is directly proportional to the square of the sound speed. Thus, if the sound speed is increased by a percent  $\delta_c$  so that the new speed is  $c(1+\delta_c)$ , the ratio of the temperature to the molecular mass must increase by a percent  $(1+\delta_c)^2-1$ . A 10% increment in the sound speed corresponds to a 21% increase in the ratio of temperature to molecular mass, and it may occur as a temperature increase from 60 km to 100 km, with a mixture of density decrease and temperature increase above

100 km. The lower panel of Figure 4 shows the effective speed predicted for the perturbed model, and Table 5 shows the predicted propagation parameters. Note the trim of high speed on the outer edge of the slowness plane, which corresponds to the first arrivals for the April 23 event. The 10% correction in the sound speed is about 8% higher than would be expected for temperature corrections in the MLT. We conclude that our assumptions on the path of propagation to IS59 and FAI are in error, and that the heterogeneity of the atmosphere may play a significant factor in the scattering of sound waves during long-range propagation.

We can still use the effective propagation speeds to compute the robustness of the location algorithm. Using the three stations, a new location and origin time are computed from the new propagation speeds, and this location is referred to as LA2. Using the same values provided in Table 5, we also compute locations using only two stations. LA3 was computed using IS59 and IS57, and LA4 was computed using IS57 and FAI. Table 6 provides the origin time and location of these solutions. Solutions LA2, LA3, and LA4 are almost identical, differing by a few seconds and only a tenth of a degree in latitude. However, the nature of the solution for the location is quite different. The aim of computing the residues is to extract the minimum, and although the residue surface for LA2 has a clearly defined minimum, the minimum for LA3 is a linear feature. This topology of the LA3 solution for the residue surface, caused by a lack of constraint perpendicular to the line between the stations, leads to instability in the location algorithm.

The only difference in the procedure used to compute the location solutions LA1, LA1b, and LA2 is in the atmospheric models. LA1 used a model where the stratospheric winds were not sufficiently strong, and this led to slow propagation and thus a predicted origin time that was too early. The predicted epicentral location was not too far off, but this match was fortuitous. LA1b had a stronger stratospheric wind, which produced a good match for IS57 and brought the origin time closer to the LO1 values, but placed the source too far northwest because of the relatively slow propagation speeds of the thermospheric phases. Solution LA2 obtained with the modified atmospheric profiles provided the best fit to LO1, as expected. The difference between LO1 and LA2 is 202 s,  $0.20^\circ$  in latitude, and  $0.61^\circ$  in longitude. This would correspond to an epicentral range of  $\sim 70$  km from the source location observed by the satellites. However, the LA2 location was obtained with perturbations in the sound speed that are unrealistic, and thus we are compelled to consider alternative explanations for the rather fast propagation speed for the IS59 and FAI arrivals.

Figure 5 shows the effective propagation speed surfaces computed at every height and slowness bin for propagation to IS59 and to IS57. A duct exists in the upper troposphere and lower stratosphere, and in a homogeneous, perfectly stratified atmosphere energy would be trapped in this duct. However, heterogeneity in the troposphere may induce scattering of the ducted energy into the ground. This hypothesis may explain the fast effective propagation speeds, the slow apparent phase speeds, and the azimuth deviations observed in directions opposite to the dominant stratospheric winds (Kulichkov, 1998). Thus, a combination of ray and scattering theories may provide a reasonable explanation for the observed arrivals.

## **CONCLUSIONS AND RECOMMENDATIONS**

Arrival times for infrasonic propagation along the dominant stratospheric winds matched well the predicted arrivals, but unreasonable modifications to the sound speed profile in the upper atmosphere were needed to match the arrival times of possible thermospheric phases. Ongoing studies concentrate on the propagation of acoustic energy in leaky ducts in the troposphere and stratosphere. Further work should also quantify the scales of inhomogeneity and the degree of acoustic scattering in the atmosphere up to heights of 150 km.

## **REFERENCES**

- Garces, M, D. Drob, M. Picone, K. Lindquist, and R. Hansen (2000). Characterization Of Infrasonic Waves Observed In Hawaii During Summer, 22<sup>nd</sup> Seismic Research Symposium: Planning for Verification of and Compliance with The Comprehensive Nuclear-Test-Ban Treaty, New Orleans.
- Garcés, M. A., R. A. Hansen, and K. Lindquist (1998). Travel times for infrasonic waves propagating in a stratified atmosphere, *Geophys. J. International*, 135, 255-263.

Kulichkov, S. N. (1998). On problems of infrasonic monitoring of small energy explosions, Proceedings of the Informal Workshop on Infrasound, Bruyeres-Le-Chatel, France.

**Table 1. Station location, range from LO1, and azimuth from LO1 for April 23, 2001 bolide event.**

Station	Latitude	Longitude	Range, km	Azimuth, deg
IS57	33.60	-116.50	1777.7	253.8262
IS59	19.59	-155.9	2419.0	63.4996
FAI	64.87	-147.84	4228.7	159.7367

**Table 2. Observed array parameters: arrival azimuth, slowness (ray parameter) in s/km, and estimated time of arrival of the first coherent energy packet.**

Station	Azimuth, deg	Slowness (s/degree)	ETA (UT)
IS57	249.0	316.8	07:48:40 +/- 45 s
IS59	65.6	338.4	08:20:14 +/- 45 s
FAI	143.1	423.0	10:12:13 +/- 45 s

(Used conversion factor of 111.1949266 km/degree)

Station	Slowness (s/km)	Speed (km/s)	ETA (Epoch time)
IS57	2.8491	0.3510	988012120 +/- 45 s
IS59	3.0433	0.3286	988014056 +/- 45 s
FAI	3.8041	0.2629	988020733 +/- 45 s

**Table 3. Apparent slowness, apparent speed, and azimuth deviation of infrasonic detections for LO1.**

Station	App. Slowness (T/X, s/km)	App. Speed (X/T, km/s)	Azimuth deviation
IS57	3.2430	0.3084	4.8262
IS59	3.1835	0.3141	-2.1004
FAI	3.4001	0.2941	16.6367

**Table 4. Predicted apparent slowness, apparent speed, and azimuth deviation for unmodified meteorological model.**

Station	App. Slowness (T/X, s/km)	App. Speed (X/T, km/s)	Azimuth deviation	Turning Height (km)
IS57	3.27	0.305 (Is)	0.8	48
IS59	3.57	0.280 (It)	-1.0	117
FAI	3.70	0.270 (It)	-0.5	115

**Table 5. Predicted apparent slowness, apparent speed, and azimuth deviation for modified meteorological model.**

Station	App. Slowness (T/X, s/km)	App. Speed (X/T, km/s)	Azimuth deviation	Turning Height (km)
IS57	3.27	0.305	0.8	48
IS59	3.33	0.300	-1.3	112
FAI	3.48	0.287	-0.5	112

**Table 6. Source Origin Time and Location.**

Source ID	Origin time	Latitude (N)	Longitude (W)
LO1	988006355	27.9	133.89
LA1	988005598	29.5	134.9
LA1b	988005878	29.6	136.0
LA2	988006153	28.2	134.5
LA3	988006152	28.1	134.5
LA4	988006167	28.2	134.5

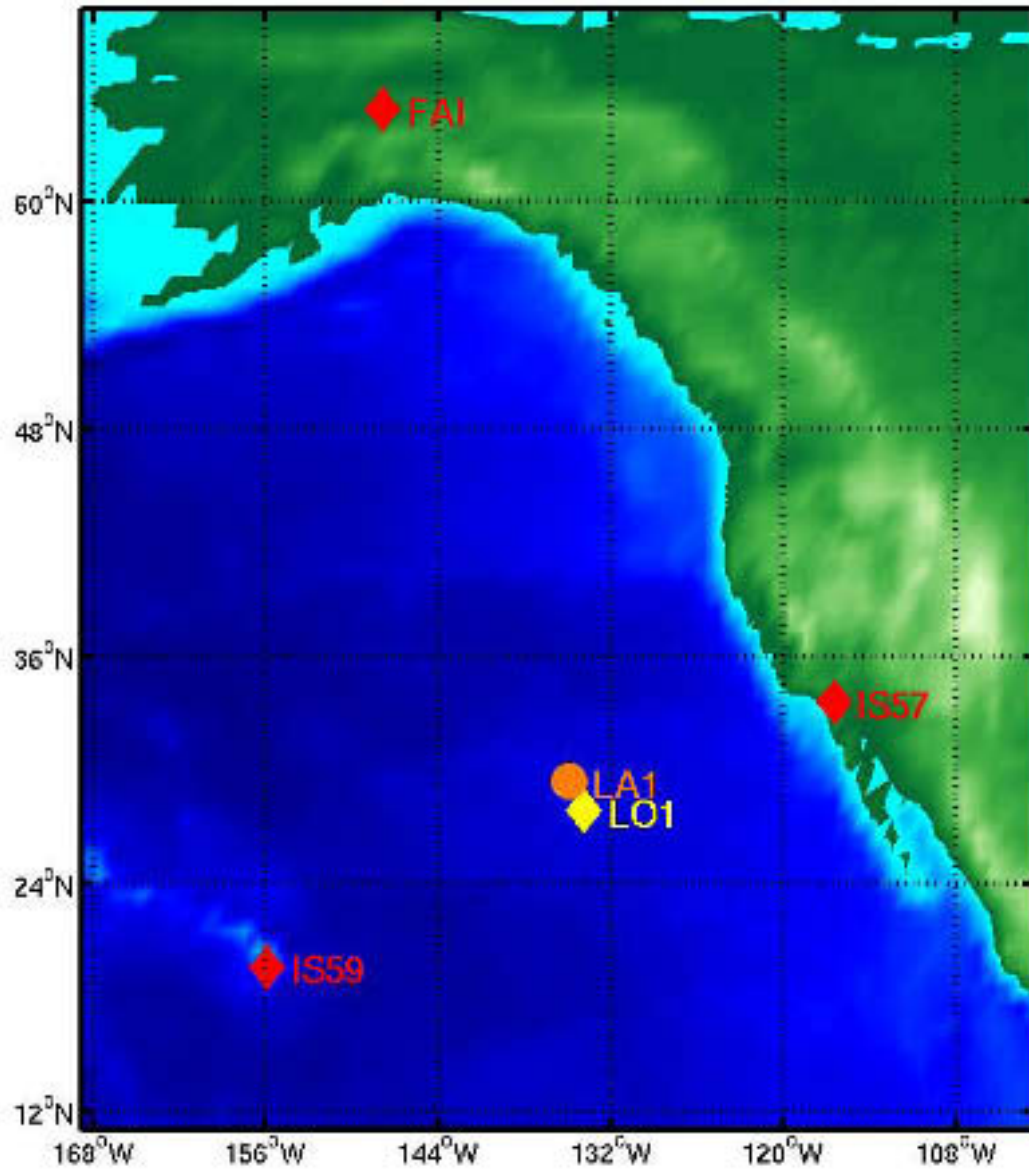


**Figure 1.** Location of infrasound monitoring station IS59, IS57, and FAI. LO01 shows the source location determined by US satellites, and LA01 shows the first location determined from ray tracing within one week of the event detection. In addition to the three arrays shown, the LA1 location used DLIAR and IS10.

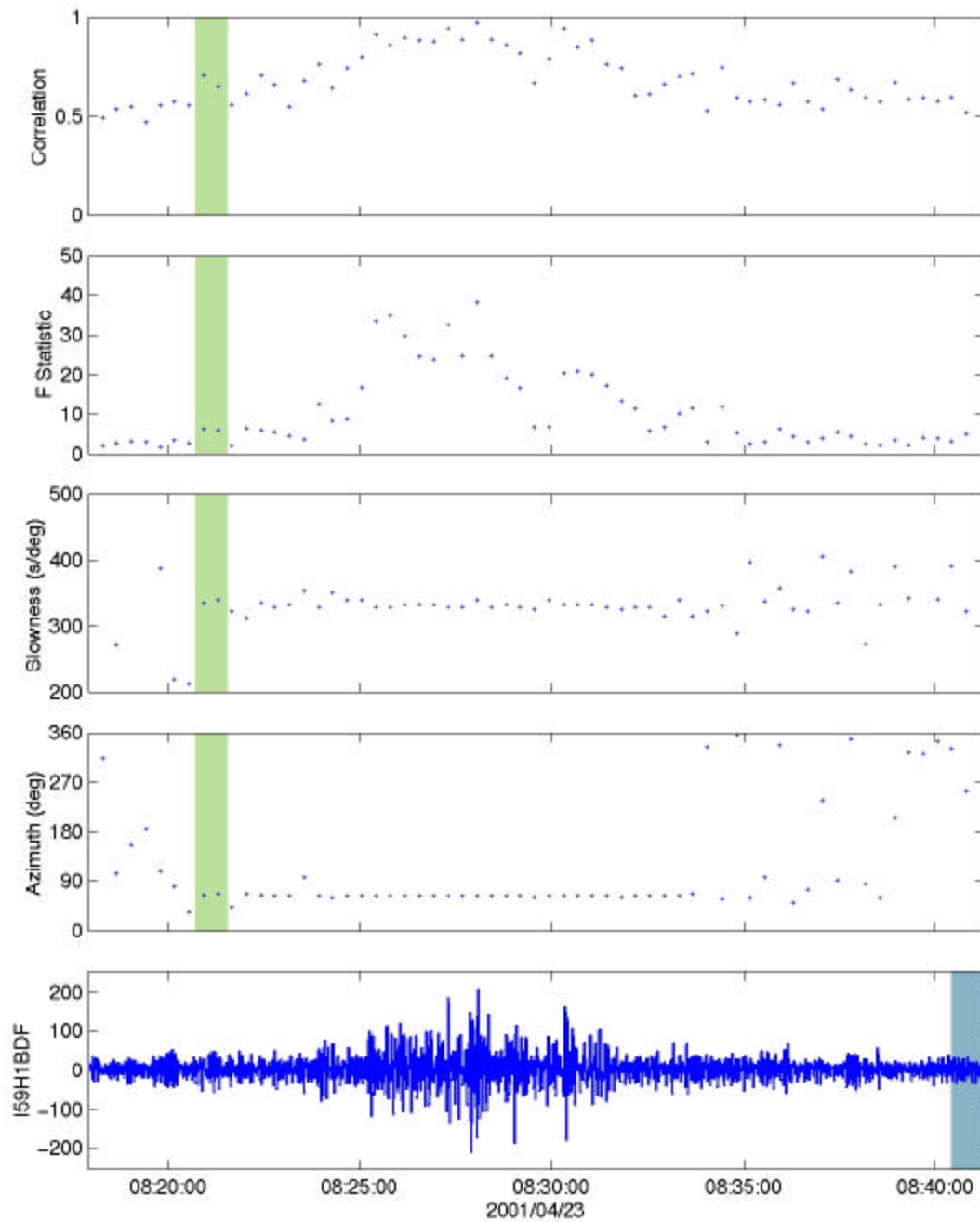


Figure 2. Detection of the April 23 bolide at IS59, Hawaii.

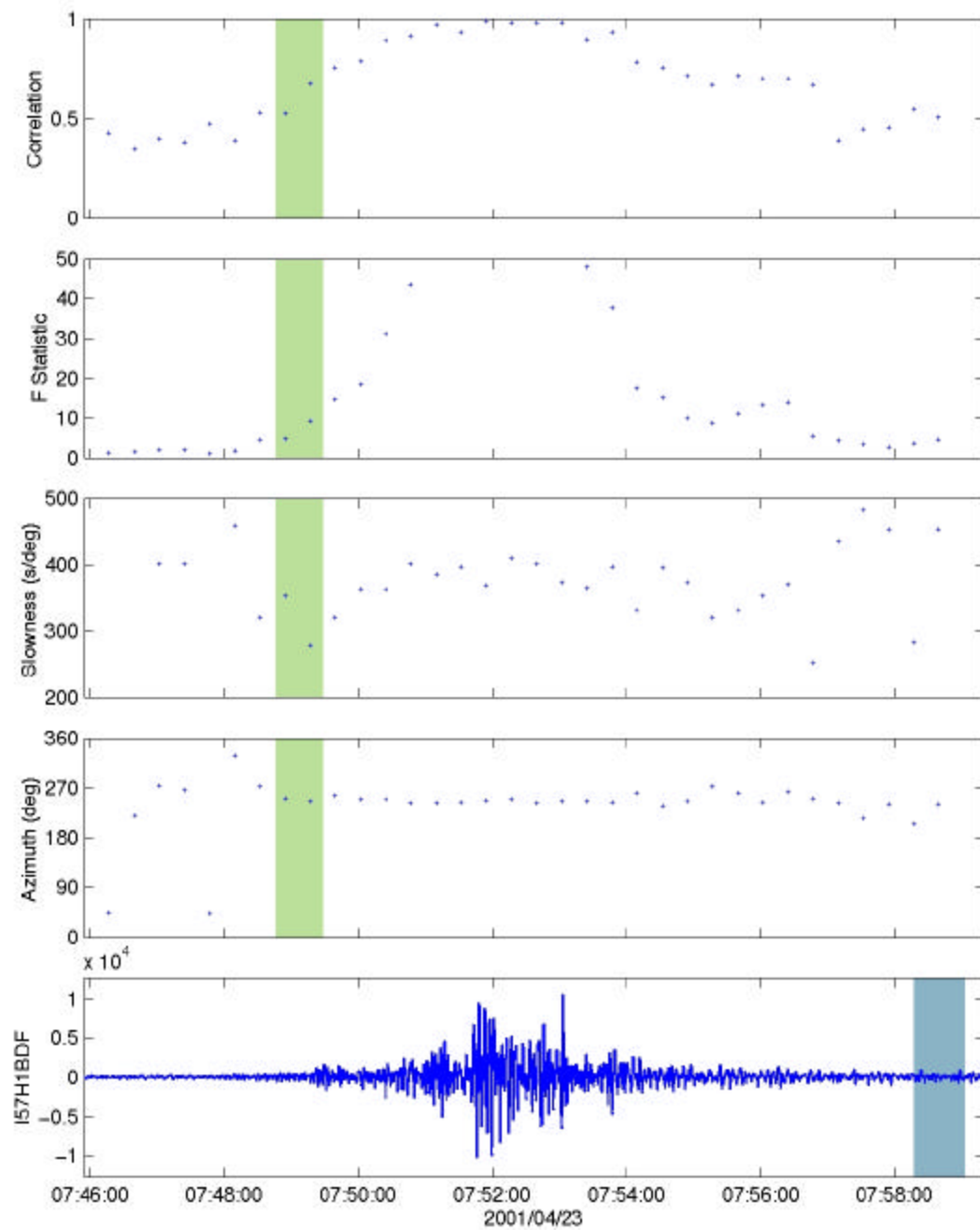
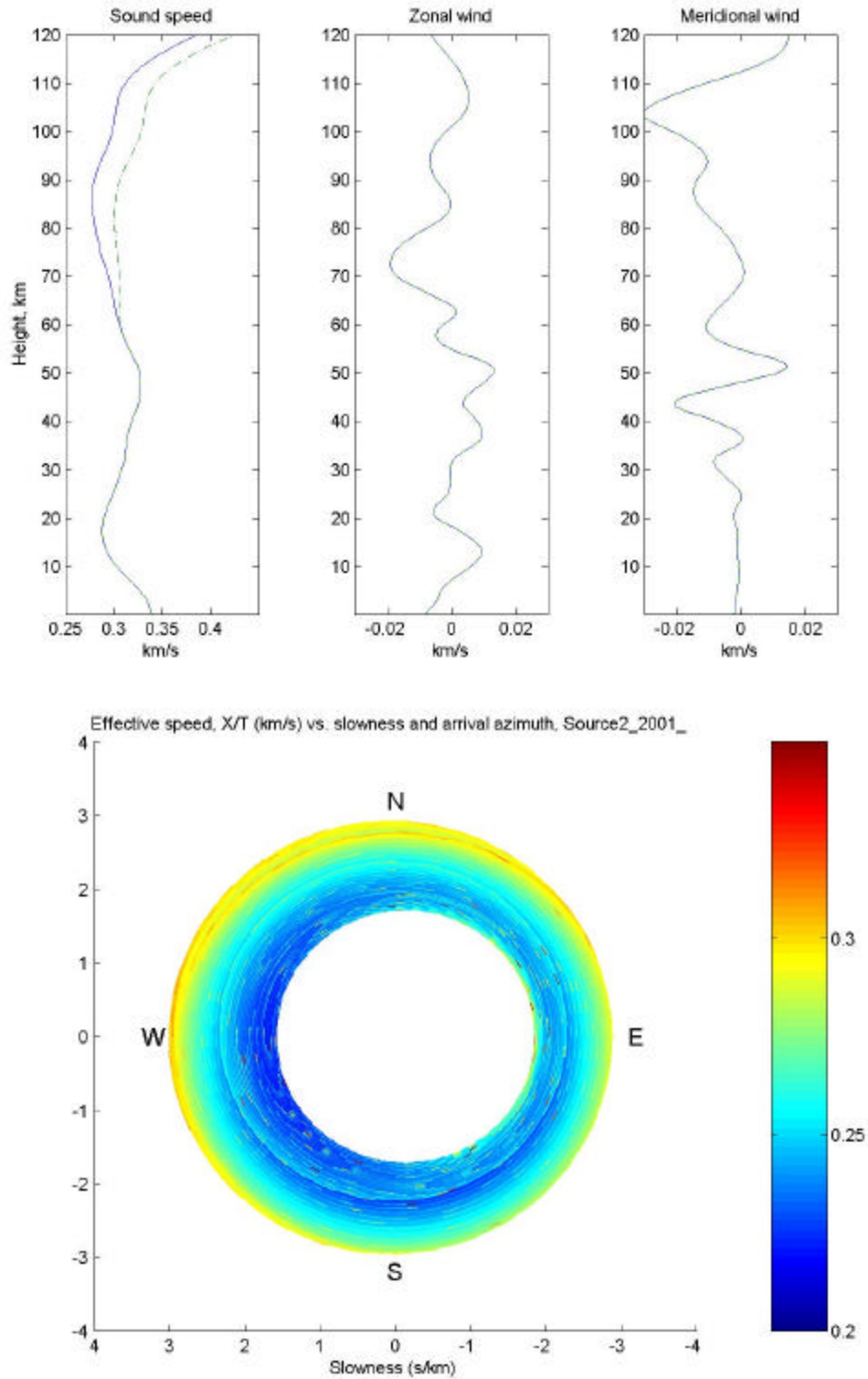
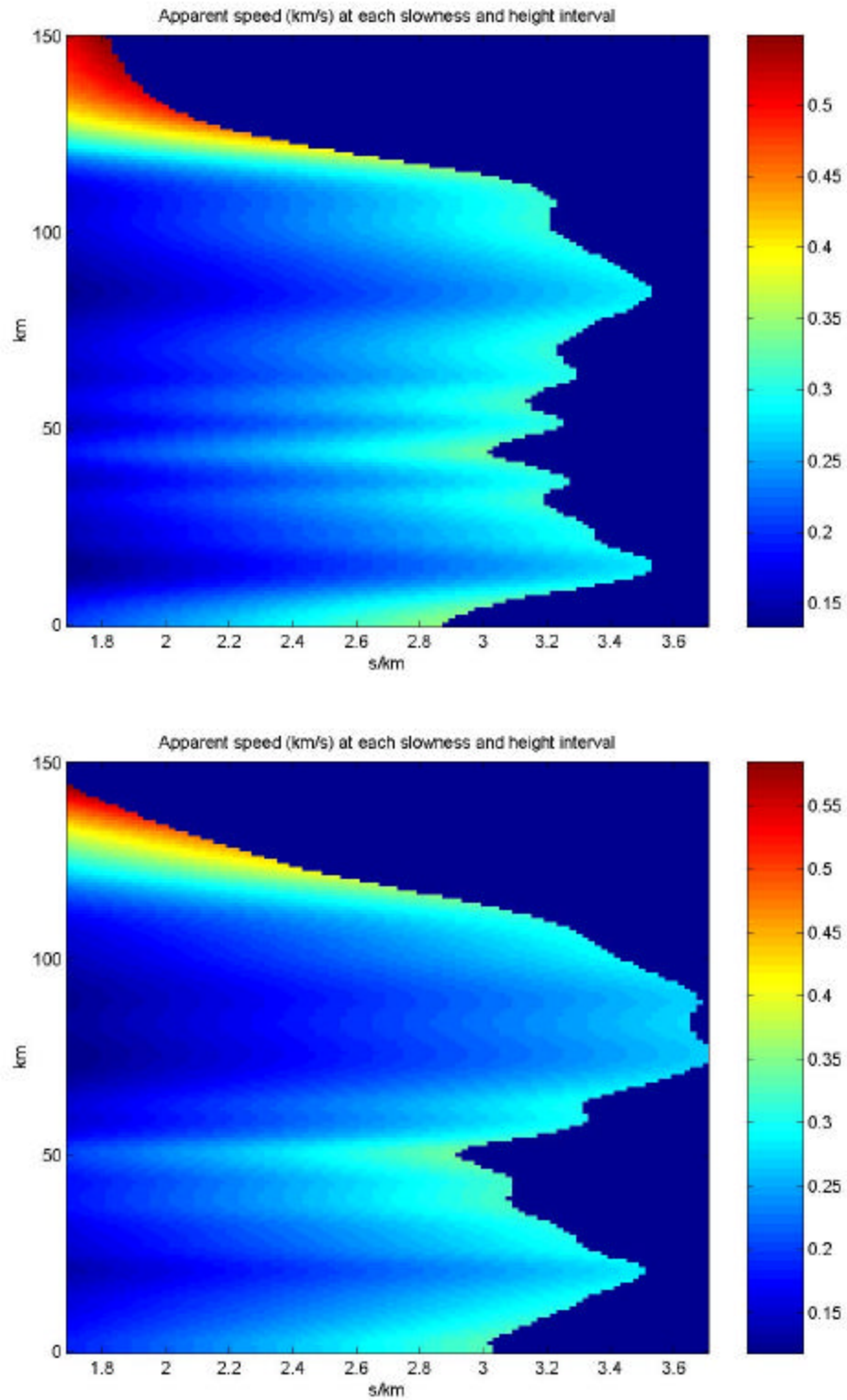


Figure 3. Detection of the April 23 bolide at IS57, Pinon Flat, CA.



**Figure 4.** Atmospheric profiles and predicted effective propagation speed. The dashed line denotes the modified atmospheric sound speed, and the effective speed is computed using the perturbed profiles. Note the high-speed trim on the edge of the slowness plane.



**Figure 5.** Effective speed (range over travel time) at each height and slowness interval for IS59 (above) and IS57 (below). The stratospheric phase for IS57 at 3 s/km is well defined. A duct exists between 10 and 50 km, and that this energy may be scattered into the ground.